Experimental Silicosis

Morphologic and Biochemical Abnormalities Produced by Intratracheal Instillation of Quartz Into Guinea Pig Lungs

James H. Dauber, MD, Milton D. Rossman, MD,
Giuseppe G. Pietra, MD, Sergio A. Jimenez, MD,
and Ronald P. Daniele, MD

Six months after intratracheal instillation of silica, histologic, ultrastructural, cytologic, and biochemical studies were performed on the lungs of guinea pigs. The tissue response consisted of both diffuse alveolar septal infiltration with interstitial fibrosis and granulomatous infiltration with nodular fibrosis. Ultrastructural studies confirmed the presence of a mixed inflammatory exudate in the alveolar interstitium (histiocytes, neutrophils, eosinophils, and lymphocytes) and the Type II lining of cell hyperplasia. The number of lung cells recovered by lavage and the proportions of neutrophils and multinucleated cells in bronchoalveolar cells were significantly greater in experimental animals ($P < .05$) than in controls (intratracheal saline). Total lung collagen and collagen synthesis by cultured lung tissue were also increased in the experimental animals. Since the response of guinea pig lung to intratracheal silica included pathologic features common to human silicosis and idiopathic pulmonary fibrosis, this model has the potential for improving our understanding of both of these important clinical disorders. (Am J Pathol 1980, 101:595-612)

ALTHOUGH INTENSIVE efforts have been made in the last 50 years to elucidate the pathogenesis of silicosis, the events leading to the accumulation of inflammatory cells and collagen in the lungs of animals and humans exposed to silica are only partially understood. Since silicosis continues to be a clinically important occupational lung disease, further attempts to improve our understanding of its pathogenesis are warranted. In order to examine the inflammatory and fibrotic reaction to inhaled silica in a systematic manner, we have produced experimental silicosis in the guinea pig. The purpose of this report is to describe changes in the lung and thoracic lymph nodes of animals that have been exposed to quartz by intratracheal instillation.

The results of our histologic, cytologic, ultrastructural, and biochemical

---

From the Department of Medicine, Cardiovascular-Pulmonary Division and Section of Rheumatology, and the Department of Pathology, University of Pennsylvania School of Medicine, Philadelphia, Pennsylvania.

Supported by Young Investigator Awards 1R23-HL-21134 (Dr. Dauber) and 1R23-HL-24500 (Dr. Rossman), Research Career Development Award 1K04-HL-00210 (Dr. Daniele), and Grant R01-HL-23877 from the National Heart, Lung, and Blood Institute.

Accepted for publication June 27, 1980.

Address reprint requests to James H. Dauber, MD, Cardiovascular-Pulmonary Division, Box 678, Hospital of the University of Pennsylvania, 3400 Spruce Street, Philadelphia, PA 19104.

0002-9440/80/1209-0595$01.00

studies indicate that characteristic patterns of inflammation and fibrosis regularly occur in animals 6 months after exposure to silica by this route. Thus, this model should prove to be a valuable tool for elucidating the pathogenesis of pulmonary inflammation and fibrosis in general and silicosis in particular. Our findings also suggest that this model may improve our understanding of the events leading to fibrosis in other forms of interstitial lung disease.

Materials and Methods

Animals

Hartley outbred strain male guinea pigs (West Jersey Biologicals, Wenonah, NJ) weighing between 300 and 500 g were observed for 1 week prior to intratracheal injection for signs of illness. They were housed in open quarters during the entire study.

Silica Particles

Silica particles were prepared from a sample of Min-U-Sil, 5 μ (Pennsylvania Glass Sand Corporation, Pittsburgh, Pa). To remove the Fe_2O_3 that may contaminate these particles, a 3% (wt/vol) slurry was boiled in 1 N HCl until the green color disappeared.[1] Particles were washed 4 times in large volumes of distilled water to remove chloride. A 1% slurry was sedimented and centrifuged to remove excessively small and large particles. The size distribution of the injected silica as determined by scanning electron microscopy was: < 1 μ, 21%; 1–2 μ, 35%; 2–3 μ, 30%; 3–4 μ, 11%; 4–5 μ 3%; > 5 μ, 0% (Dr. V. Damiano, Franklin Institute, Philadelphia, Pa, personal communication). Particles were sterilized by heating at 200 C for 2 hours.

Animal Protocol

The results presented herein were derived from 4 cohorts of animals. Each cohort contained an experimental (intratracheal silica) and a control (intratracheal saline) group. The animals in each cohort received their intratracheal injection on the same day, but the cohorts were given injections at different times during the course of the study. Each animal was injected only once. For the experimental animals, the dose of silica was 50 mg suspended in 1 ml of sterile saline. Control animals received 1 ml of sterile saline.

All injections were made by the transtracheal route. The trachea was exposed surgically with animals under light ether anesthesia, and the silica suspension or saline was briskly injected through a curved 25-guage needle in order to achieve as uniform a distribution as possible.[2]

Surviving animals were sacrificed 6 months after injection. At this time a thoractomy was performed under pentobarbital anesthesia, and the animal was exsanguinated by direct cardiac puncture. The heart and lungs were removed *en bloc* and examined grossly before being used for study. The 6-month observation period was chosen because it has been reported that nodular fibrosis usually develops by this time in the lungs of guinea pigs that have been exposed to silica by the intratracheal route.[3]

Morphologic Studies

Fixation and Gross Examination of Lungs

The lungs were fixed by intratracheal instillation of 10% formalin or Bouin's solution. After the lungs had been fully expanded by the instilled fixative, the trachea was tied and

the lungs immersed in fixative for 4 or 18 hours. At this time, the right upper, right lower, left upper, and left lower lobes were removed from their bronchi and cut serially in the sagittal plane. These sections were examined for evidence of consolidation. Lungs from 9 experimental and 5 control animals were prepared in this way.

Histologic Examination

Portions of tracheobronchial lymph nodes and the midline sagittal sections from the right upper, right lower, left upper, and left lower lobes were fixed for an additional 18 hours in Bouin's solution before being embedded in paraffin. Sections 6 μ thick were cut and stained with hematoxylin and eosin, Mallory trichrome, and reticulin (modified Foot's) stain. Selected sections were also stained with Ziehl-Nielson, Grocott, Gram, and Alizarin Red-S stains.

Lungs from 3 experimental and 2 control animals were fixed *in situ* by vascular perfusion as described in detail elsewhere.[4] Small cubes of tissue were cut from the fixed lungs and embedded in Epon. Sections 1 μ thick were stained with methylene blue.

Ultrastructural Examination

Lung tissue from one experimental animal was prepared for study by transmission electron microscopy. These lungs were fixed by the intratracheal instillation of 2.5% glutaraldehyde in 0.1 M sodium cacodylate buffer. Fixation time was 2 hours. Small tissue blocks were cut, postfixed in 1% OsO_4, dehydrated in ascending grades of acetone, embedded in Spurr's resin, and cut with a diamond knife. Sections with a thickness that produced silver interference color were cut, mounted on copper grids, stained with lead hydroxide and uranyl acetate, and examined with a Siemens (Elmiskop 101) electron microscope. Specimens from the remaining lung tissue were fixed an additional 18 hours in Bouin's solution and prepared for light-microscopic examination as described in the previous section. The histologic abnormalities seen in these lungs were similar to those seen in lungs from other experimental animals. Thus, the tissue used for ultrastructural analysis was representative of the experimental group.

Cytologic Studies

Lung cells were obtained by lavage of the right lung from 6 experimental and 5 control animals in a standard manner described previously[5] except that the left mainstem bronchus was clamped and the lungs massaged after each aliquot of fluid was aspirated. Because the initial 15 ml of lavage fluid recovered from experimental and control animals contained a substantial number of ciliated epithelial cells and nonviable cells, it was discarded. Lavage was continued until 100 ml of fluid was recovered. Lavage fluid was centrifuged at 500*g* at 4 C for 10 minutes. The supernatant was removed and the cell pellet washed twice in Ca^{++}–Mg^{++}-free Hanks' balanced salt solution (HBSS) (Grand Island Biological Company [GIBCO], Grand Island, NY). The pellet was resuspended in RPMI 1640 medium (GIBCO) and the total cell count made on a Model Z_F Coulter Counter (Coulter Electronics, Hialeah, Fla). Viability was determined by exclusion of trypan blue. Smears for differential counting were made with a cytocentrifuge (Shandon Southern Corp., Sewickley, Pa) and stained with Diff-Quik (Harleco, Philadelphia, Pa) and for nonspecific cytoplasmic esterase with the use of α-naphthyl-butyrate as substrate.[6] The occurrence of multinucleated giant cells in bronchoalveolar cells was quantified in two ways: First, as the proportion of macrophages that contained 2 or more nuclei and, second, as the fusion index. This index was obtained by dividing the number of nuclei within multinucleated cells in a given area by the total number of nuclei within the same area.[7] The result was multiplied by 100 and expressed as a percentage.

Biochemical Studies

Collagen Content of Lungs

We estimated the total lung collagen from the hydroxyproline content, assuming that the imino acid represented 14% of the collagen molecule. Major bronchi were dissected, and the remaining lung parenchyma finely minced. The minced parenchyma was homogenized in a measured volume of 1 M NaCl buffered to pH 7.4 with 0.05 M Tris-HCl. An aliquot of this homogenate was hydrolyzed in 6 N HCl at 125 C for 16 hours. Hydroxyproline in the hydrolysate was assayed by the colorimetric method of Prockop and Udenfriend.[8]

The amount of collagen in both lungs (total lung collagen) was determined in 7 experimental and 6 control animals. In Cohort 2 (3 experimental and 3 control animals), the content of the right and left lung was measured individually, and the results added to give total lung collagen. In Cohort 3 (4 experimental and 3 control animals), tissue from the two lungs of each animal was combined before being homogenized and assayed for total lung collagen.

Protein and Collagen Synthesis by Cultured Lung Tissue

Samples of approximately 100 mg were selected from the minced lung used in the collagen content assay described above. They were incubated as previously described[9] in Krebs-Ringer solution containing 20 mM HEPES, 20 mM glucose, 20 μg/ml ampicillin and 5 μCi/ml of uniformly labeled ^{14}C-proline (285 μCi/μmole, New England Nuclear, Boston, Mass) for 18 hours at 37 C with gentle shaking and then homogenized in the culture medium. The homogenate was extensively dialyzed against running tap water to eliminate unincorporated ^{14}C-proline. Aliquots of the dialyzed homogenate were hydrolyzed as described above, and we determined incorporation of ^{14}C-proline by counting an aliquot of the hydrolysate in a liquid scintillation spectrometer. The ^{14}C-hydroxyproline present in collagen was determined by the method of Juva and Prockop.[10] Protein and collagen synthesis was expressed as the mean ± SE counts per minute of incorporated ^{14}C-proline and ^{14}C-hydroxyproline, respectively, in the replicate samples of tissue from each lung.

Samples of the left lung from 3 experimental and 3 control animals were examined in this way.

Statistics

The Student *t* test was used to determine the significance of the differences between mean values for experimental and control animals.

Results

Animal Survival and Utilization

The results presented in this report were derived from animals sacrificed 6 months after intratracheal injection. Prior to sacrifice, however, spontaneous deaths occurred in both the experimental and control animals. Approximately 50% of experimental animals had died before the 6-month observation period elapsed (Table 1). More than half of these animals were dead within 3 weeks of the injection. The lungs of these animals were firm and dark red. Hemorrhagic fluid exuded from their cut surfaces. Because more than 12 hours had elapsed before autopsies were performed

Table 1—Animal Survival and Utilization

Cohort Number	Survival*		Histology		Cytology†		Total lung collagen		Collagen synthesis‡	
	Si	C	Si	C	Si	C	Si	C	Si	C
1	3/3	2/2	3	2	3	2	ND		ND	
2	4/9	8/9	1	1	3	3	3	3	3	3
3	6/18	4/5	1	ND§	ND		4	3	ND	
4	8/10	4/4	7	4	ND		ND		ND	
Total	21/40	18/20	12	7	6	5	7	6	3	3

* Number of animals surviving at 6 months/total number of animals injected for the group. Si, experimental animals; C, control animals.

† Cells obtained by lavaging the right lung only.

‡ Synthesis of collagen and total protein by fragments of the left lung *in vitro*.

§ ND = not done.

on the unpreserved cadavers, histologic sections of lung were not prepared. The lungs of the 2 control animals that died spontaneously appeared grossly normal.

The studies performed on the lungs from injected animals are also shown in Table 1. In some cases, the same lung was used for more than one study. The right lung of the animals in Cohort 2 was lavaged prior to determination of collagen content, while samples of the left lung were taken for biosynthetic studies before the remainder of the tissue was homogenized for collagen content determination. Histologic sections were prepared from both lavaged (right) and unlavaged (left) lungs in Cohort 1. Although the histologic abnormalities were similar in sections from lavaged and unlavaged lungs, the changes described below represent what was observed in unlavaged lungs.

Response of the Lung to Injected Silica

Gross Findings

Firm nodules as large as 5 mm were present on the pleural surface of the majority of lungs examined. Nodules were palpated in the perihilar region of at least one lobe of all experimental animals. Peribronchial consolidation was evident on the cut surface of at least 2 out of 4 major lobes from 12 experimenatl animals (Figure 1). Occasionally, consolidation was more diffuse and extensive, involving greater than half of the cut surface of the lobes. Consolidated areas were pale and firm. In no case did they resemble the hemorrhagic type seen in the animals that died spontaneously. Lungs from control animals appeared normal.

Microscopic Findings

In areas where the lungs were grossly consolidated, extensive cellular infiltrates surrounded the central airways (Figure 2A) and often extended out to pleural surface. Smaller infiltrates occurred less commonly around distal bronchioles. Infiltration was more prominent in the lower lobes of 6 animals, but in the other 3 the upper lobes were more involved.

Two patterns of infiltration of the alveolar interstitial space were appreciated. In the first, the infiltrating cells formed granulomas, while in the second they were not organized and usually did not greatly distort alveoli. The granulomas consisted almost entirely of histiocytes. A few granulomas contained scattered foci of lymphocytes. Multinucleated giant cells were occasionally seen in or around the granulomas. In the lungs of about a third of the animals the central regions of a few granulomas were undergoing necrosis. These necrotic areas contained silica particles identified by their typical appearance and ability to polarize light, but special stains failed to demonstrate the presence of acid-fast organisms, fungi, or bacteria. Some of the necrotic areas contained calcium.

Diffuse infiltration of alveolar septa occurred in the parenchyma surrounding the granuloma (Figure 2A). Histiocytes were again the most prominent inflammatory cell; but neutrophils, eosinophils, and lymphocytes were also present. The severity of septal infiltration varied. In some areas, the number of inflammatory cells was few and the architecture of the alveolus well preserved. On the other hand, some septa were heavily infiltrated and the alveoli quite distorted. In most, however, the intensity of infiltration fell between these extremes. Some lungs contained areas of diffuse interstitial infiltration in which no granulomas were visible, but this was not the rule (Figure 2B). The alveolar air spaces in regions of diffuse infiltration contained large mononuclear cells that were probably macrophages, substantial numbers of multinucleated giant cells (Figure 2C), and a few neutrophils.

Infiltrated alveoli were almost invariably lined by metaplastic epithelial cells, which, in most cases, had the appearance of Type II pneumocytes (Figure 2C). The air spaces adjacent to granulomas, however, were frequently lined by ciliated columnar cells, which were probably derived from bronchial epithelium (Figure 3A). Occasionally, these cells lined air spaces in areas of diffuse infiltration where granulomas were not seen.

Sections from lungs fixed by vascular perfusion contained the same types of abnormalities described above and thus corroborated the results of the histologic analysis of lungs fixed by intratracheal instillation.

Three patterns of collagen deposition were noted on trichrome-stained sections. Some of the granulomas had hyalinized central regions in which strands of collagen were arranged in a concentric fashion (Figure 3A);

these granulomas resembled early silicotic nodules. Thin strands of collagen were almost invariably detected in the interstitium of diffusely infiltrated alveoli (Figure 3B). Thick bands of collagen were occasionally encountered in peribronchial granulomas (Figure 3C) and in densely infiltrated alveolar septa. Sections stained for reticulin revealed increased amounts in the septa of infiltrated alveoli and a network of dense fibers surrounding the histiocytes in the granulomas.

The lungs of all but one of the control animals were normal on microscopic inspection. There were several small foci of chronic inflammatory cells in the right lung of this animal, which probably were infectious in origin. However, no granulomas or fibrosis was seen in these inflamed areas.

Transmission Electron Microscopy

Lymphocytes, plasma cells, macrophages, neutrophils, eosinophils, and increased amounts of collagen were found in the septa of infiltrated alveoli (Figure 4A). In addition, the cuboidal alveolar lining cells contained abundant lamellar bodies indicating that Type II cell hyperplasia had indeed occurred (Figure 4B). Thus, the ultrastructural evaluation confirmed one of the important findings of the histologic studies, namely, that there is interstitial fibrosis associated wtih a mixed cellular infiltrate and Type II cell hyperplasia in the lungs of experimental animals.

Although it was not always apparent on light-microscopic sections, most of the histiocytes in the granulomas contained silica particles (Figure 5A). Many of the particles were enclosed within membranes, but a few appeared to lie free in the cytoplasm. Particles were occasionally seen outside cells. The majority of the mononuclear cells in alveolar spaces appeared to be macrophages which also frequently contained ingested silica (Figure 5B).

Lavage Studies

The number of bronchoalveolar cells obtained by a standard lavage from the experimental animals was substantially higher than from the controls ($[71 \pm 11$ vs. $32 \pm 6] \times 10^6$ cells, mean $\pm$ SE, $.03 < P < .04$). Viability of cells was similar, 92% vs 93%, respectively. Differential counts for experimental and control animals differed in two respects. First, there was a threefold increase in the proportion of neutrophils in experimental animals (Text-figure 1). Second, the proportion of multinucleated cells was also increased in this group (14 ± 1.0 vs. 5 ± 0.9%, mean $\pm$ SE, $P < .001$). Multinucleated giant cells from experimental animals contained a greater number of nuclei than giant cells from control animals. This finding was

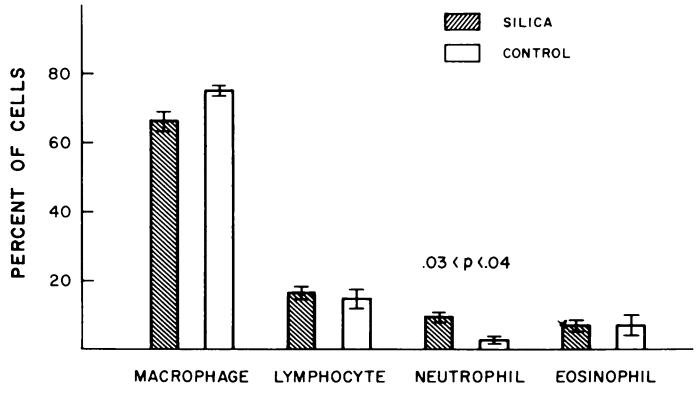

TEXT-FIGURE 1—Differential count of bronchoalveolar cells. The values represent the mean ± SE for experimental and 5 control animals. Neutrophils were more frequent in experimental animals, compared with control animals (9 ± 1.7 vs. 3 ± 1.5% $P < .04$). Differences in the proportions of macrophages, lymphocytes, and eosinophils were not statistically significant ($P > .20$ in all cases).

corroborated by the high fusion index for experimental animals (34 ± 3.7 vs. 10 ± 2.8%, $P < .001$). Approximately 75% of multinucleated cells from experimental animals contained silica particles, which were identified not only visually but also by electron probe analysis (Dr. V. Damiano, Franklin Institute, Philadelphia, Pa, personal communication).

Biochemical Studies

Lung Collagen

The lung collagen content for experimental animals was more than double that for the control animals (Table 2). Although there was considerable variation in this value, it should be noted that the lowest value for experimental animals exceeded the highest value for control animals. In addition, the value for experimental animals, which had been injected at different times, was similar (Cohorts 2 and 3).

For 2 of the 3 animals in Cohort 2, the collagen content of the right lung exceeded that of the left (data not shown). The mean values for the content of the right and left lung, however, were nearly identical, 65.4 ± 1.1 vs 63.0 ± 18.0 mg (mean ± 1 SE), respectively.

The wet weight of the left lung of experimental animals in Cohort 2 was almost double that of control animals (4.12 ± .21 vs 2.49 ± 0.03 g, mean ± 1 SE, $.001 < P < .002$). The fraction of wet lung weight due to collagen was also higher in the experimental animals, but the difference between mean values for the two groups was not statistically significant (Table 2).

Table 2—Collagen Content of Lungs

Cohort number	Total lung collagen* (mg)		Collagen fraction† (mg/g lung‡)	
	Control	Silica	Control	Silica
2	41.2	116.5	8.04	14.5
	76.0	163.9	15.4	18.1
	37.8	104.2	7.6	13.6
3	78.9	96.9	ND	ND
	43.1	123.7		
	75.3	200.1		
		117.6		
Mean ± SE	58.7 ± 8.1	132 ± 14	10.3 ± 2.5	15.4 ± 1.3
P	.001< *P*<.002		.20< *P*<.25	

* Content of the left and the right lung.
† Values represent fractions for the left lung only.
‡ Wet lung weight.

Protein and Collagen Synthesis

Both total protein synthesis, measured by incorporation of ^{14}C-proline into macromolecules, and collagen synthesis, measured by the formation of ^{14}C-hydroxyproline, were substantially higher in cultures of lung tissue from experimental animals, compared with control animals (Table 3).

Response of Tracheobronchial Lymph Nodes

Grossly, these nodes were firm and markedly enlarged, measuring up to 1.5 cm. Microscopically, the medullary sinusoids and lymphoid follicles were intensely infiltrated by histiocytes, but these cells had not organized

Table 3—Protein and Collagen Synthesis *In Vitro**

	Total protein synthesis† (^{14}C-proline cpm × 10^{-6})		Collagen synthesis† (^{14}C-hydroxyproline cpm × 10^{-5})		Number of samples cultured from each lung
	Control	Silica	Control	Silica	
	142	211	14.0	21.4	4
	72	172	9.8	28.3	2
	80	178	11.0	35.3	4
Mean ± SE	98 ± 22	187 ± 12	11.6 ± 1.2	28.3 ± 4.0	
	.02< *P*<.025		.020< *P*<.025		

* All data were derived from Cohort 2.
† Mean ± SE for replicate samples from one lung.

into granulomas, as they had done in the lung. Many of the histiocytes were multinucleated. The severity of fibrosis varied, but in all nodes examined, there were at least several small hyalinized foci containing strands of stainable collagen. At the center of some fibrotic areas there was degeneration and necrosis similar to that seen in the lung. Again, special stains failed to identify acid-fast organisms, fungi, or bacteria.

Discussion

These studies showed that three patterns of pulmonary fibrosis, ie, nodular, interstitial, and peribronchial, consistently developed in guinea pigs within six months of an intratracheal injection of quartz particles. The development of nodular and peribronchial fibrosis following inhalation [11] and tracheal injection [3] of silica has been well documented. These patterns resemble the type of fibrosis seen in human silicosis.[11]

Of equal interest is the pattern of diffuse interstitial fibrosis. It has been observed in several animal species with experimental silicosis [3] but has received less attention than the other patterns. The interstitial fibrosis in our study was invariably associated with an interstitial infiltrate consisting of macrophages, lymphocytes, and granulocytes and usually with an alveolar infiltrate consisting of macrophages, giant cells, and neutrophils. Epithelial metaplasia, Type II lining cell hyperplasia in particular, was prominent. Thus, the reaction to injected silica in these animals included some of the histologic features of human idiopathic pulmonary fibrosis. In addition, an increase in the proportion of neutrophils in lavaged cells was seen in these animals. A similar finding has been reported for human idiopathic pulmonary fibrosis.[12]

It is generally agreed that a successful model of diffuse idiopathic pulmonary fibrosis should possess most of the morphologic features that are considered characteristic for human disease.[13] These include: *a*) a mixed cellular exudate in the interstitium, *b*) epithelial metaplasia, *c*) a protein exudate in the air spaces, with or without leukocytes, *d*) gradual progression to fibrosis and honeycombing, *e*) continuing activity even when partly fibrotic, *f*) a diffuse distribution with no localization around airways, and *g*) areas of spared parenchyma (skip zones). In this study we have demonstrated that the reaction in guinea pig lung 6 months after insufflation of silica includes most of the features of the ideal animal model listed above. Exceptions to these criteria in our model are that the reaction occurred around airways and that honeycombing was not apparent. Localization of the reaction around the airways probably is due to the route of exposure to silica (intratracheal injection). Whether honeycombing will eventually develop cannot be determined from this study. Since the fibrotic reaction

in these animals will probably progress,[3] it is possible that honeycombing will be seen in animals that received silica 9–12 months before being sacrificed. In addition to possessing most of the histologic features of diffuse interstitial fibrosis, this response was highly reproducible, occurring in all experimental animals examined. Thus, we believe that this model shows considerable potential for providing new information about the pathogenesis of diffuse idiopathic pulmonary fibrosis.

Total lung collagen was greatly elevated in the silicotic animals, as was the amount of stainable collagen. Collagen accumulation in tissue may result from enhanced synthesis, diminished degradation, or a combination of these mechanisms. Since samples of lung from experimental animals produced increased amounts of hydroxyproline *in vitro*, it is likely that enhanced synthesis is one pathway leading to pulmonary fibrosis in this form of silicosis. Although the fraction of wet lung weight due to collagen was not significantly greater in experimental animals, compared with controls, the number of samples was small. Thus, it cannot be definitely concluded that the collagen fraction is not increased in this form of pulmonary fibrosis. Failure to demonstrate an increased collagen fraction, however, has been reported for silica-induced fibrosis in guinea pigs,[14] bleomycin-induced fibrosis in baboons,[15] and idiopathic fibrosis in man.[16]

Accumulation of other substances such as noncollagen proteins,[14,15] water,[14,15] and lipids [17] probably also contributed to the increase in lung weight. The increase due to retained silica was insignificant. In view of the extensive infiltrates on histologic sections and the large number of cells recovered by lavage, a portion of the increase in lung weight must also be due to the accumulation of inflammatory cells in alveoli and the interstitium.

Gardener was one of the first investigators to draw attention to the nature of the cellular response in experimental silicosis.[11] He described an influx of both neutrophils and macrophages after silica deposited in the air spaces but emphasized the predominance of the latter. The cellular reaction at this stage of the response in our animals also consisted primarily of macrophages and histiocytes. The presence of neutrophils in the histologic sections and the increased numbers of these cells recovered by lavage suggest, however, that polymorphonuclear leukocytes were also being recruited to the silicotic lung. Increased numbers of multinucleated giant cells were also found in the lungs and lavage fluid of the silicotic guinea pigs. The origins and functions of giant cells are poorly defined. The ease with which large numbers of them can be recovered from silicotic animals may facilitate studies designed to examine these points. It should be emphasized that although we did not quantify the constituents of the cellular

reaction in the lung, the composition of the bronchoalveolar cells mirrored the composition of the interstitial infiltrate. This finding lends further support to the concept that the composition of cells recovered by lung lavage may be an indication of the type and severity of interstitial lung disease.[12,18–20]

In summary, we have shown that intratracheal instillation of silica is a reliable method for producing pulmonary inflammation and fibrosis in guinea pigs. The inflammatory and fibrotic response resembles what is seen not only in silicosis but also in idiopathic pulmonary fibrosis. Thus, this model appears to have the potential for improving our understanding of both the fibrogenic action of silica and the mechanisms leading to the accumulation of inflammatory cells and collagen in diffuse interstitial lung disease.

References

1. Allison AC: Fluorescence microscopy of lymphocytes and mononuclear phagocytes and the use of silica to eliminate the latter, In Vitro Methods in Cell-Mediated and Tumor Immunity. Edited by BR Bloom, and JR David. New York, Academic Press, 1976, pp 395–404
2. Goldstein B, Webster I, Sichel HS: Evaluation of experimental methods in the determination of the fibrogenic action of dust: I. The intratracheal method. Br J Exp Pathol 1962, 43:38–43
3. Zaidi SH: Experimental Pneumoconiosis. Baltimore, Johns Hopkins University Press, 1969, pp 69–79
4. Gil J, Weibel ER: Morphologic study of pressure-volume hysteresis in rat lungs fixed by vascular perfusion. Respir Physiol 1972, 15:190–213
5. Dauber JH, Daniele RP: Chemotactic activity of guinea pig alveolar macrophages. Am Rev Respir Dis 1978, 117:673–684
6. Li CY, Lam KW, Yam LT: Esterase in human leukocytes. J Histochem Cytochem 1973, 21:1–12
7. Warfel AH: Macrophage fusion and multinucleated giant cell formation, surface morphology. Exp Mol Pathol 1978, 28:163–176
8. Prockop DJ, Udenfriend S: A specific method for the analysis of hydroxyproline in tissues and urine. Anal Biochem 1960, 1:228–239
9. Jimenez SA, Yankowski RI, Frontino PM: Biosynthetic heterogeneity of scleroderma tous skin in organ cultures. J Mol Med 1977, 2:423–430
10. Juva K, Prockop DJ: Modified procedure for the assay of H^3– or C^{14}– labeled hydroxyproline. Anal Biochem 1966, 15:77–83
11. Gardener LU: General tissue responses to various kinds of mineral particles, Silicosis and Asbestosis. Edited by AJ Lanza. New York, Oxford University Press, 1938, pp 277–282
12. Reynolds HY, Fulmer JD, Kazmierowski JA, Roberts WC, Frank MM, Crystal RG: Analysis of cellular and protein content of broncho-alveolar lavage fluid from patients with idiopathic pulmonary fibrosis and chronic hypersensitivity pneumonitis. J Clin Invest 1977, 59:165–175
13. Carrington CB: Organizing interstitial pneumonia: Definition of the lesion and attempts to devise an experimental model. Yale J Biol Med 1968, 40:352–363
14. Bailey P, Kilroe-Smith TA, Harrington JS: Biochemistry of lungs in relation to sili-

cosis: II. The effect of quartz dust on protein amino acids of guinea pig lung tissue. Arch Environ Health 1964, 8:547–554
15. McCullough B, Collins JF, Johanson WG, Grover FL: Bleomycin-induced diffuse interstitial pulmonary fibrosis in baboons. J Clin Invest 1978, 61:79–88
16. Crystal RG, Fulmer JD, Roberts WC, Moss ML, Line BR, Reynolds HY: Idiopathic pulmonary fibrosis: Clinical, histologic, radiographic, physiologic, scintigraphic, cytologic and biochemical aspects. Ann Intern Med 1976, 85:769–788
17. Grünspan M, Antwieler H, Dehnen W: Effect of silica on phospholipids in the rat lung. Br J Indus Med 1973, 30:74–77
18. Hunninghake GW, Fulmer JD, Young RC Jr, Gadek JE, Crystal RG: Localization of the immune response in sarcoidosis. Am Rev Respir Dis 1979, 120:49–58
19. Dauber JH, Rossman MD, Daniele RP: Bronchoalveolar cell populations in acute sarcoidosis: Observations in smoking and non-smoking patients. J Lab Clin Med 1979, 94:862–871
20. Haslam PL, Turton CWG, Heard B, Lukoszek A, Collins JV, Salsbury AJ, Turner-Warwick M: Bronchoalveolar lavage in pulmonary fibrosis: Comparison of cells obtained with lung biopsy and clinical features. Thorax 1980, 35:9–18

Acknowledgments

The authors would like to thank Ms. Lynne Uhl, Ms. Angel Cassizzi, Ms. Lynette McMillan, and Ms. Melanie Minda for their assistance in preparing the animals, cells, and tissues used in these studies; Dr. Juan Gil and Ms. Judy McNiff for the preparation of lungs fixed by vascular perfusion; Mr. Ron Yankowski and Mr. Rob Klaus for their assistance in performing the biochemical determinations; and Mr. William Fore for preparing the photographs. In addition, we thank Dr. A. P. Fishman for critically reviewing the manuscript. Special thanks to Ms. Mary McNichol for her assistance in preparing the manuscript.

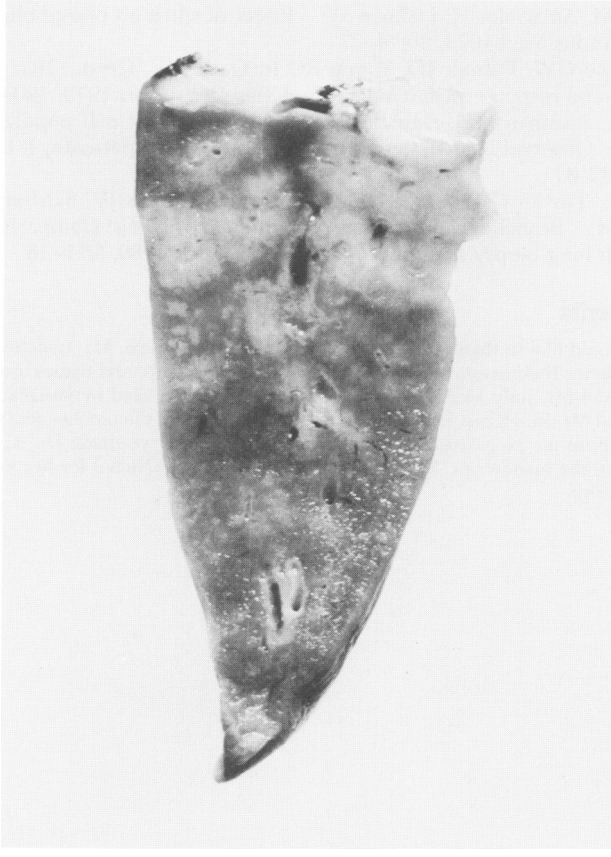

Figure 1—The cut surface of the right lower lobe from an experimental animal. Consolidation surrounds many of the central airways and extends to the pleural surface. Smaller areas of consolidation are detectable around more peripheral airways. This example is representative of the extent and distribution of consolidation in the lower lobes of experimental animals.

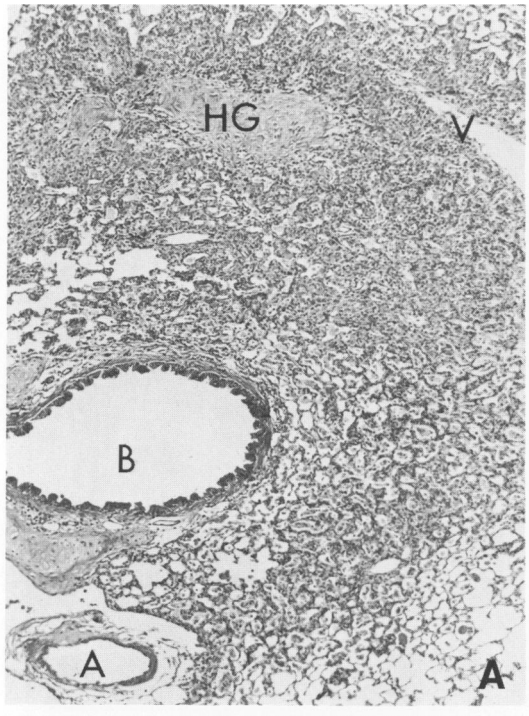

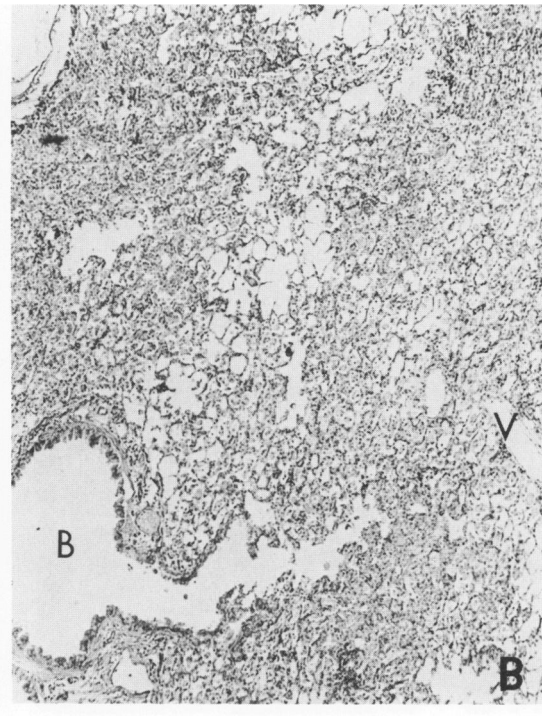

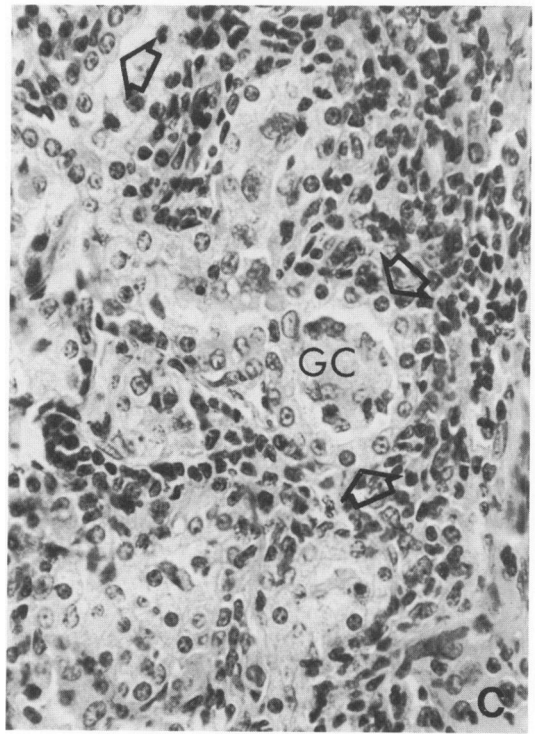

Figure 2A—A peribronchial infiltrate containing granulomas with hyalinized central regions (*HG*). The parenchyma surrounding the granulomas is diffusely infiltrated. Other abbreviations: *B*, bronchus; *A*, pulmonary artery; *V*, pulmonary vein. (H&E, ×57) **B**—A peribronchial infiltrate in which no granulomas are visible. The diffuse alveolar and interstitial infiltrate is identical to that which surrounds the granulomas in Figure 1. See text for description. (H&E, ×45) **C**—Higher magnification of a diffusely infiltrated area. In the center of the plate, a multinucleated giant cell (*GC*) fills an alveolus. Prominent cuboidal cells (*open arrowheads*) having the appearance of Type II pneumocytes line this and adjacent air spaces (H&E, ×480) (With a photographic reduction of 15%)

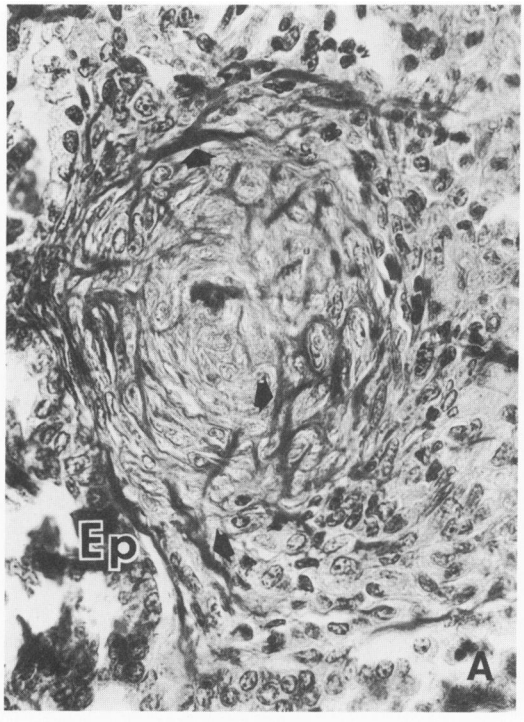

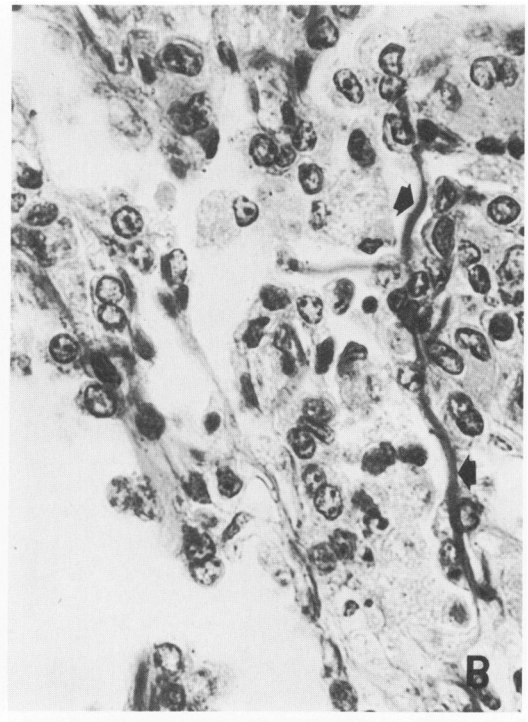

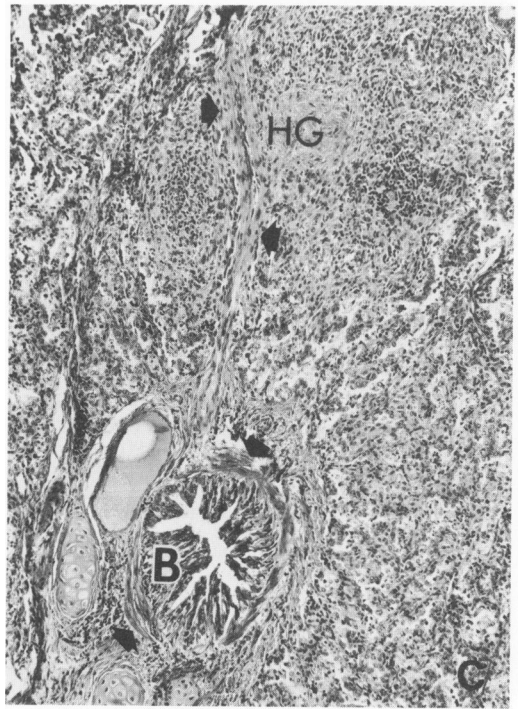

Figure 3A—Hyalinized region of a granuloma in which collagen appears as dark bands (*arrowheads*). Bronchiolar epithelial cells (*Ep*) line the air space to the left of the granuloma. These cells are thought to gain access to alveoli by ways of the pores of Lambert. (Mallory trichrome, ×320) **B**—High magnification of an area of interstitial infiltrate. Collagen fibers in the alveolar septa appear as dark strands (*arrowheads*). (Mallory Trichrome, ×720) **C**—Peribronchial fibrosis. A thick band of collagen (*arrowheads*) surrounds this bronchus (*B*) and projects into a hyalinized granuloma (*HG*). (H&E, ×90) (With a photographic reduction of 15%)

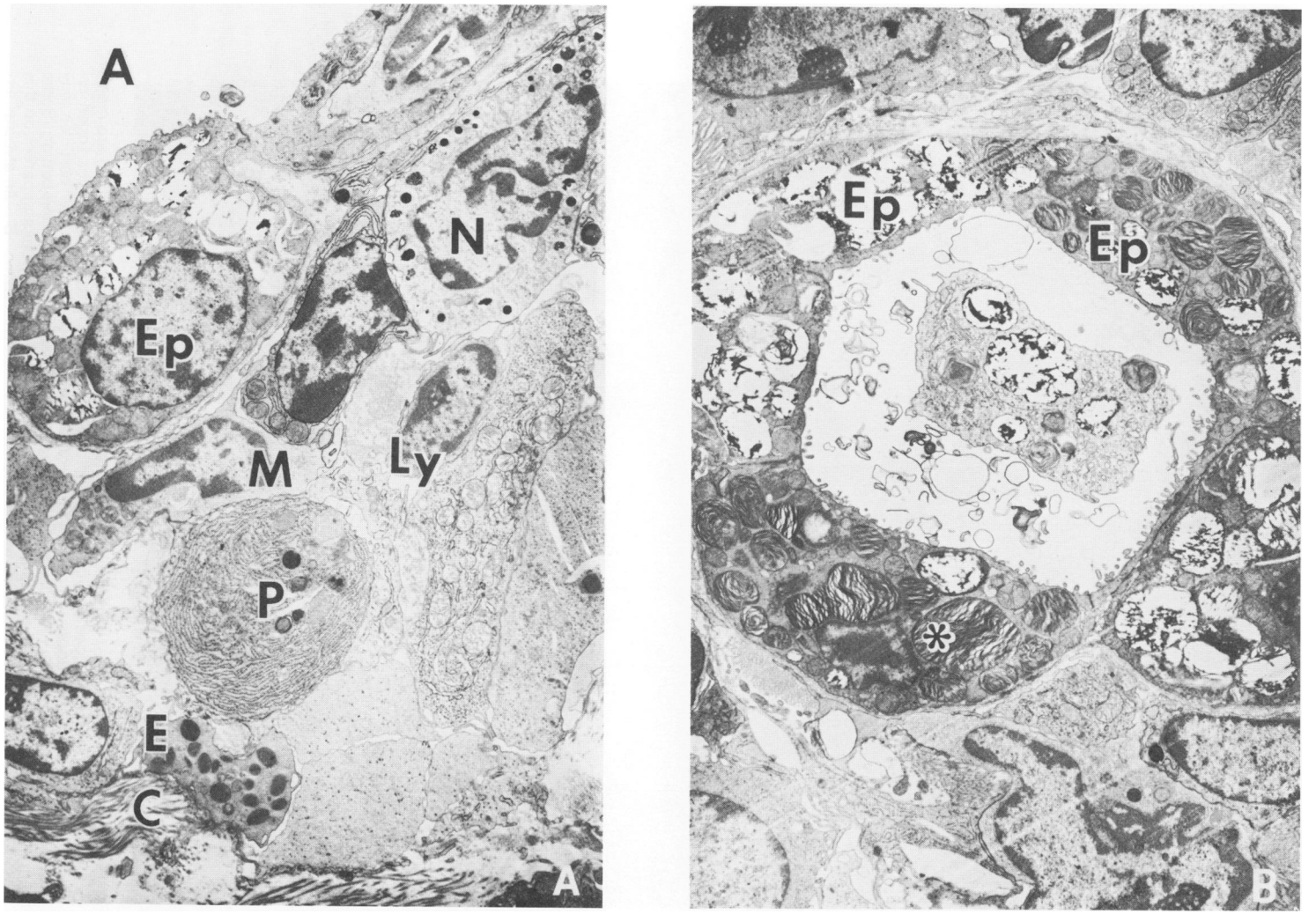

Figure 4A—Transmission electron micrograph depicting the constituents of the interstitial infiltrate. Abbreviations: *A*, alveolar airspace, *C*, collagen fibers; *E*, eosinophils; *Ep*, alveolar lining cell; *Ly*, lymphocyte; *M*, macrophage; *N*, neutrophil; *P*, plasma cell. (×4000) **B**—Large cuboidal cells (*Ep*) with numerous lamellar bodies (*) line an alveolus in an area of interstitial infiltration. This appearance is typical of Type II lining cell hyperplasia. (×4000)

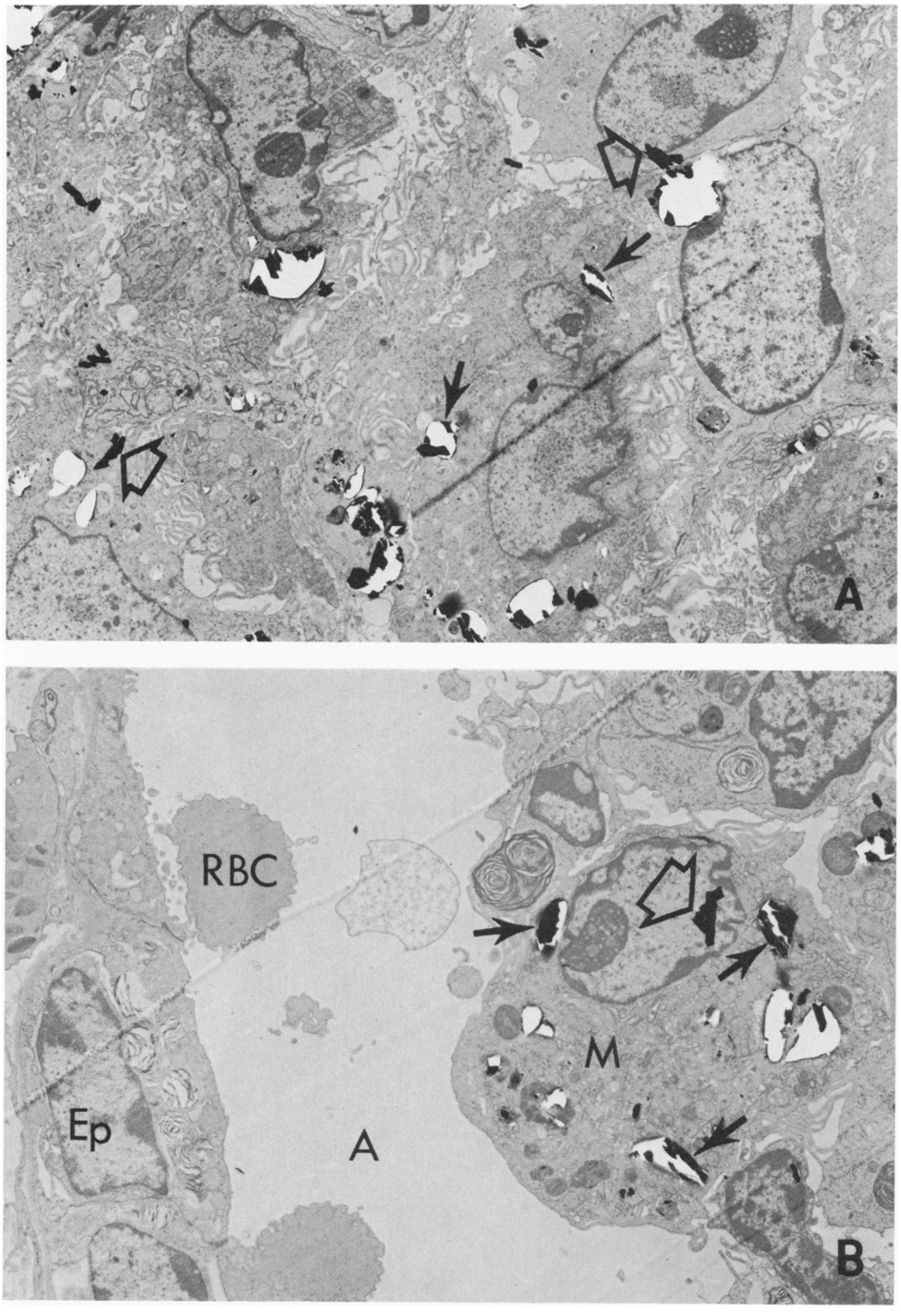

Figure 5A—A granuloma. Most of the cells contain electron-dense silica particles which are membrane-bound. A membrane does not appear to enclose several of the smaller particles (*open arrowheads*), and some even appear to occupy an extracellular location. These "free" particles may be an artifact, however. Many of the large particles appear to have fractured during cutting. Some of the fragments were dragged across the section, producing the linear streaks apparent on this and other plates (Figure 4B), and deposited outside of the cells. (×3000) **B**—An alveolar airspace (*A*) containing erythrocytes (*RBC*) and macrophages (*M*). Several electron-dense silica particles, enclosed in membranes (*arrows*), are present in one of the macrophages. The "free" particle overlying the nucleus of this cell (*open arrowhead*) probably is an artifact (for reasons discussed above).